

Article

Phase Behavior of Aqueous Mixtures of Sodium Alginate with Fish Gelatin: Effects of pH and Ionic Strength

Daria S. Kolotova ^{1,*}, Ekaterina V. Borovinskaya ¹, Vlada V. Bordiyan ¹, Yuriy F. Zuev ^{2,3} , Vadim V. Salnikov ² , Olga S. Zueva ⁴  and Svetlana R. Derkach ^{1,*} 

¹ Laboratory of Chemistry and Technology of Marine Bioresources, Institute of Natural Science and Technology, Murmansk State Technical University, Murmansk 183010, Russia; shibekoev2@mstu.edu.ru (E.V.B.); bordiyanvv@mstu.edu.ru (V.V.B.)

² Kazan Institute of Biochemistry and Biophysics, FRC Kazan Scientific Center of RAS, Kazan 420111, Russia; yufzuev@mail.ru (Y.F.Z.); vadim.salnikov.56@mail.ru (V.V.S.)

³ A. Butlerov Chemical Institute, Kazan Federal University, Kazan 420008, Russia

⁴ Institute of Electric Power Engineering and Electronics, Kazan State Power Engineering University, Kazan 420066, Russia; ostefzueva@mail.ru

* Correspondence: kolotovads@mstu.edu.ru (D.S.K.); derkachsr@mstu.edu.ru (S.R.D.)

Abstract: The phase behavior of aqueous mixtures of fish gelatin (FG) and sodium alginate (SA) and complex coacervation phenomena depending on pH, ionic strength, and cation type (Na^+ , Ca^{2+}) were studied by turbidimetric acid titration, UV spectrophotometry, dynamic light scattering, transmission electron microscopy and scanning electron microscopy for different mass ratios of sodium alginate and gelatin ($Z = 0.01\text{--}1.00$). The boundary pH values determining the formation and dissociation of SA-FG complexes were measured, and we found that the formation of soluble SA-FG complexes occurs in the transition from neutral (pH_c) to acidic ($\text{pH}_{\varphi 1}$) conditions. Insoluble complexes formed below $\text{pH}_{\varphi 1}$ separate into distinct phases, and the phenomenon of complex coacervation is thus observed. Formation of the highest number of insoluble SA-FG complexes, based on the value of the absorption maximum, is observed at pH_{opt} and results from strong electrostatic interactions. Then, visible aggregation occurs, and dissociation of the complexes is observed when the next boundary, $\text{pH}_{\varphi 2}$, is reached. As Z increases in the range of SA-FG mass ratios from 0.01 to 1.00, the boundary values of pH_c , $\text{pH}_{\varphi 1}$, pH_{opt} , and $\text{pH}_{\varphi 2}$ become more acidic, shifting from 7.0 to 4.6, from 6.8 to 4.3, from 6.6 to 2.8, and from 6.0 to 2.7, respectively. An increase in ionic strength leads to suppression of the electrostatic interaction between the FG and SA molecules, and no complex coacervation is observed at NaCl and CaCl_2 concentrations of 50 to 200 mM.

Keywords: fish gelatin; sodium alginate; polyelectrolyte complexes; complex coacervation; effect of pH; ionic strength



Citation: Kolotova, D.S.; Borovinskaya, E.V.; Bordiyan, V.V.; Zuev, Y.F.; Salnikov, V.V.; Zueva, O.S.; Derkach, S.R. Phase Behavior of Aqueous Mixtures of Sodium Alginate with Fish Gelatin: Effects of pH and Ionic Strength. *Polymers* **2023**, *15*, 2253. <https://doi.org/10.3390/polym15102253>

Academic Editor: Lacramioara Rusu

Received: 18 April 2023

Revised: 7 May 2023

Accepted: 8 May 2023

Published: 10 May 2023



Copyright: © 2023 by the authors. Licensee MDPI, Basel, Switzerland. This article is an open access article distributed under the terms and conditions of the Creative Commons Attribution (CC BY) license (<https://creativecommons.org/licenses/by/4.0/>).

1. Introduction

Interactions between proteins and polysaccharides have been actively studied in previous decades due to the widespread application of these compounds in food technologies, the cosmetic industry, medicine, pharmaceuticals, tissue engineering, and many other fields [1–8]. In particular, proteins are used as emulsifying, foaming, gelling, or structuring agents in the food industry to develop liquid or solid matrices of functional food products [9] and in drug delivery systems [10] and for the creation of films, coatings, and capsules in the food, pharmaceutical, and cosmetic industries [11–13]. Polysaccharides are also widely used in many industries as thickeners or moisture-retaining, gelling, drying, or structuring agents [14–16].

Depending on internal and external factors, the interaction between proteins and polysaccharides in aqueous media can adopt two directions: either attraction or repulsion [17,18]. Such factors include the molecular characteristics of proteins and polysaccharides (molecular weight, conformation, chain flexibility, type and number of reaction

groups, chain charge density); solvent properties (pH, ionic strength, polarity); and mixing conditions (temperature, time, pressure, ratio of protein and polysaccharide, total concentration of biopolymers, presence of crosslinking agents) [17,19–21].

Attractive interactions between proteins and polysaccharides occur mainly due to electrostatic interactions between positively charged protein groups and negatively charged polysaccharide groups [19,21,22]. Such interactions lead to the formation of soluble or insoluble protein–polysaccharide complexes. The insoluble complexes then separate, forming a two-phase system consisting of the phases containing the complexes and the solvent. This phase separation phenomenon is also called “complex coacervation” if the separated insoluble complexes are in the liquid state or “precipitation” if the complexes are in the solid state.

It is known that flexible weakly charged anionic polysaccharides, such as gum arabic, hyaluronic acid, dextran sulfate, and some pectins, tend to form liquid coacervates with positively charged proteins due to their relatively weak electrostatic interaction [21,23]. On the other hand, rigid, strongly charged anionic polysaccharides, such as gellan gum, sodium alginate, and κ -carrageenan, tend to form solid coacervates due to their stronger electrostatic attraction with proteins [17,21].

Repulsive interactions are caused by the thermodynamic incompatibility of equally charged or uncharged biopolymers [24,25].

Controlling protein–polysaccharide interactions could be a promising strategy for overcoming the disadvantages when using each biopolymer separately and improving their properties. In addition, the polyelectrolyte complex formation method is popular due to its low cost, low energy consumption, and efficiency compared with conventional processes such as solvent evaporation, emulsification, polymerization, etc. [26,27]. The formation of such non-covalent complexes does not require the use of organic solvents or crosslinking agents [28,29].

Many works have reported the interaction between proteins and polysaccharides—which are simultaneously biopolymers and polyelectrolytes—such as gelatin–hummiliarabic [30], soy protein isolate–pectin [31,32], canola protein isolate–(θ -, η - and ι -) carrageenan [33], and others. Protein–polysaccharide interactions, including the formation of polyelectrolyte complexes, have been discussed in detail in previous reviews [6,21,34]. Water-soluble polyelectrolyte complexes are formed only under strictly defined conditions (ratio of components, pH) [35,36].

Systems containing gelatin and polysaccharides of marine origin are among the most promising systems currently used in biomedicine, pharmaceuticals, and the food industry due to the high availability, low cost, safety, and biodegradability of these materials [37–39]. Gelatin, being a polyampholyte, can form complexes with both cationic and anionic polysaccharides depending on the pH of the medium. In the literature, there are many papers devoted to studying the interactions of gelatin with polysaccharides of different origins, such as gum arabic [22], sodium alginate [40], and κ -carrageenan [41]. The process of gene delivery using polyelectrolyte nanoparticles derived from cationized gelatin and anionic polysaccharides, dextran sulfate, and chondroitin sulfate was studied in [42]. Despite the fact that there are many research articles demonstrating the potential application of polyelectrolyte polysaccharide–protein complexes in drug delivery, the detailed characteristics of these materials have not yet been described. From a practical point of view, the establishment of a correlation between the structures of such complexes and their properties is particularly interesting.

Thus, the purpose of this investigation is to study the phase behavior of aqueous mixtures of sodium alginate with fish gelatin during complexation. This includes assessing the effects of pH and ionic strength on the phase behavior of SA-FG aqueous mixtures.

2. Materials and Methods

2.1. Materials

Sodium alginate from brown algae (A2033, Sigma, Gillingham, UK) was used. The average mass molecular weight of sodium alginate was determined by HPLC using an LC-20A chromatograph with a RID-10A refractive index detector (Shimadzu Corp., Kyoto, Japan) with a Shodex Asahipak GS-520 HQ and GS-620 HQ (7.5 mm × 300 mm). The molecular mass distribution of alginate was assessed by normalizing the peak areas [43]. The average mass molecular weight (M_w) of sodium alginate is ~507 kDa. The amount of alginic acid was determined on the basis of a color reaction with 3,5-dimethylphenol, and sulfuric acid was used as a reference [44]. The alginic acid content of the sodium alginate sample was $(92.2 \pm 0.7)\%$.

Fish gelatin from Atlantic Cod skin was obtained according to the method described in [45] for use in experiments. After being preliminarily cleaned from scales and residual muscle tissue, the cod skin was thawed, chopped into 5 mm × 5 mm pieces, and then treated with ethanol to remove fat. Next, the cod skin was mixed with distilled water at a ratio of 1:3 (by wt%) and stirred for 10 min. Gelatin extraction was carried out at pH = 5 for 3 h at 50 ± 1 °C with constant stirring at a speed of 80–100 rpm. The medium pH was adjusted by adding glacial acetic acid. After extraction, the reaction mixture was neutralized to pH 5.5–6.0 and then filtered by vacuum filtration at 30 °C through a paper filter with a pore diameter of 12 µm. The resulting filtrate (gelatin aqueous dispersion) was dried in a FreeZone lyophilic dryer (Labconco, USA) at -50 °C and a residual pressure of 2.4–2.6 Pa. The molecular weight of fish gelatin was determined to be 153 kDa by HPLC at a wavelength of 280 nm using the LCMS-QP8000 chromatograph (Shimadzu, Japan). The isoelectric point of gelatin (pI) was measured as 7.4 with the turbidimetric method and as 7.1 with the viscosimetric method. The amino acid composition of the gelatin is given in Table 1.

Table 1. Amino acid composition (amino acid content, g/100 g protein) of gelatin.

Amino Acids	Content, g/100 g Protein
Glycine	18.5
Proline	12.2
Hydroxyproline	7.5
Aspartic acid	5.6
Glutamic acid	9.1
Serine	6.6
Histidine	1.9
Threonine	2.7
Arginine	7.7
Alanine	9.3
Taurine	3.7
Tyrosine	1.0
Valine	2.1
Methionine	1.8
Isoleucine	1.6
Leucine	2.9
Lysine	3.5
Phenylalanine	2.3

2.2. Aqueous Mixtures of Sodium Alginate with Fish Gelatin

Aqueous dispersions of fish gelatin (FG) and sodium alginate (SA) with a concentration of 0.2 wt% were separately prepared by dissolution in distilled water overnight at 25 °C and constant stirring. Then, aqueous mixtures of alginate with gelatin were prepared by adding the SA dispersion to the FG. The mass ratio of sodium alginate and gelatin ($Z = C_{SA}/C_{FG}$, g_{SA}/g_{FG}) in the aqueous mixtures varied between 0.01 and 1.00 with a constant concentration of gelatin of $C_{FG} = 0.1$ wt%. To study the effect of pH on the

formation of SA-FG complexes, the pH of the mixtures was preliminarily adjusted to ~8 using 0.1 M NaOH. The effect of the ionic strength on the interaction of FG with SA was studied by adding sodium and calcium chlorides (1–200 mM) at $Z = 0.07$ and $C_{FG} = 0.1$ wt%.

2.3. Turbidimetric and UV Absorption Spectrum Measurements

Ultraviolet spectral measurements of pure fish gelatin, sodium alginate, and aqueous mixtures of sodium alginate and fish gelatin (SA-FG) in the wavelength range of 190 to 700 nm were recorded at 25 °C with an accuracy of 1 nm using a UV-Vis spectrophotometer T70 (PG Instruments, Wibtsoft, United Kingdom). The width of the quartz cuvette was 1 cm. The deionized water was used as a blank sample. The concentration of biopolymers in individual dispersions was 0.1 wt%. The mass ratio of SA and FG in the mixtures ranged from 0.01 to 1.00, with a constant concentration of gelatin of $C_{FG} = 0.1$ wt%.

The interaction of FG with SA was investigated using the method of turbidimetric titration. The gelatin dispersion ($C_{FG} = 0.2$ wt%) was titrated with a dispersion of sodium alginate ($C_{SA} = 0.2$ wt%). The optical density was measured at a wavelength of $\lambda = 400$ nm and an optical path length of $l = 1$ cm using a spectrophotometer T70 (PG Instruments, Wibtsoft, United Kingdom). Measurements were carried out at room temperature (25 °C).

2.4. Turbidimetric Acid Titration

The turbidimetric acid titration method was used to study the phase behavior of aqueous mixtures of FG with SA at 25 °C. To study the effect of pH on the phase behavior of SA-FG mixtures with Z from 0.01 to 1, SA-FG aqueous mixtures were titrated to pH ~2 using acetic acid solutions of different concentrations (1–100%) to minimize dilution effects. During titration, the pH and optical density values were recorded. The optical density and pH of the mixtures were determined during titration at a wavelength of $\lambda = 400$ nm and an optical path length of $l = 1$ cm using a UV-Vis spectrophotometer T70 (PG Instruments, Wibtsoft, United Kingdom) at 25 °C.

The critical pH values (pH_c , $pH_{\varphi 1}$, pH_{opt} , $pH_{\varphi 2}$) were determined from the dependence of absorbance on pH obtained during acid titration in accordance with the method described in [17,18,30], where pH_c is the limiting pH value at which there is initial weak interaction between the polymers with the formation of soluble complexes; $pH_{\varphi 1}$ is the limiting pH value below which the mixture becomes turbid due to the formation of insoluble sodium alginate–gelatin complexes; $pH_{\varphi 2}$ is the limiting pH value below which turbidity disappears due to dissociation of those complexes [18]; and pH_{opt} is the pH value at which the highest optical density was observed (Figure 1).

2.5. Particle Size Measurements

The average hydrodynamic radius of particles was measured by dynamic light scattering using the Photocor Complex-ZI analyzer (Photocor, Moscow, Russia). A thermally stabilized semiconductor laser ($\lambda = 638$ nm, 30 mW) was used as a light source. The samples were held for 1 h before measurements. Measurements of the SA-FG complexes' hydrodynamic radii were carried out at a scattering angle of 90° and temperature of 25 °C. All of the measurements were done at least in triplicate.

2.6. Zeta Potential Measurements

Zeta potential was measured using an analyzer—Photocor Complex-ZI (Photocor, Moscow, Russia)—equipped with a thermally stabilized semiconductor laser ($\lambda = 638$ nm, 30 mW) as the light source. Doppler signal analysis was performed in a mode of phase analysis light scattering (PALS). Electrophoretic mobility μE of particles was converted to zeta potential using the Smoluchowski equation. All values of zeta potential were obtained at a scattering angle of 20°. The measurements were performed at 25 °C, and the samples were held for 60 min before the measurements. All of the measurements were done at least in triplicate.

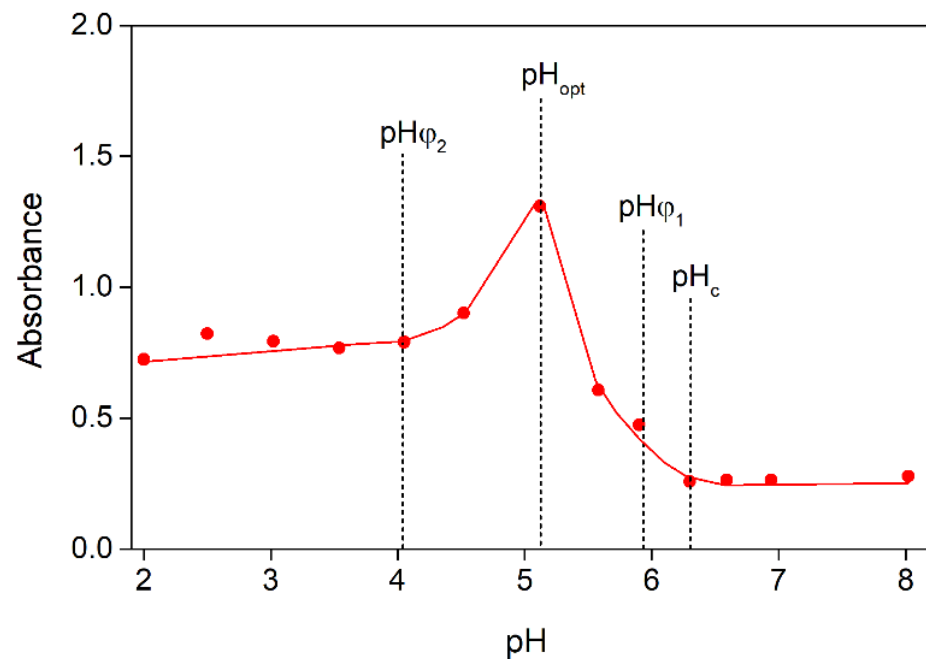


Figure 1. Changes in absorbance during the acid titration of aqueous SA-FG mixture prepared at $Z = 0.10$, where $\lambda = 400$ and $T = 25$ °C.

2.7. Scanning Electron Microscopy (SEM) and Transmission Electron Microscopy (TEM)

Field emission scanning electron microscopy multipurpose analytical complex Merlin (Carl Zeiss, Oberkochen, Germany) and an HT7700 Exalens transmission electron microscope (Hitachi, Tokyo, Japan) were used to capture images of SA-FG mixtures.

3. Results

3.1. Influence of the SA-FG Mass Ratio

The UV absorption spectra of the SA, FG dispersions, and SA-FG aqueous mixtures were obtained at a mass ratio of biopolymers, Z ($Z = C_{SA}/C_{FG}$, g_{SA}/g_{FG}), from 0.01 to 0.1 (Figure 2). In sodium alginate aqueous dispersion, the absorption maximum was observed at a wavelength of 197 nm. This is due to the presence of hydroxyl and carboxyl groups in the molecule, which absorbs in the ultraviolet range [46]. For the fish gelatin dispersion, a broad absorption band was detected at 224 nm. Undivided nitrogen electron pairs conjugated to double bonds in histidine and arginine residues [46], as well as conjugated double bonds in the benzene ring of aromatic amino acids, especially tyrosine [47], were found to contribute significantly to the absorption band position of gelatin.

It was found that the introduction of sodium alginate into the gelatin dispersion led to a shift in the maximum absorption wavelength from 220 to 229 nm, and this was accompanied by an increase in absorbance and a significant broadening of the obtained absorption band (Figure 2). The observed changes in the spectra of gelatin are associated with electrostatic interactions between charged carboxyl groups of the β -D-mannuronic and α -L-guluronic acid residues of sodium alginate and the amino groups of gelatin. These changes were also observed as a result of the formation of hydrogen bonds between hydroxyl groups of sodium alginate and tyrosine residues of gelatin. The increase in the absorption intensity in this region of the spectrum is associated with light scattering by the particles of polyelectrolyte complexes.

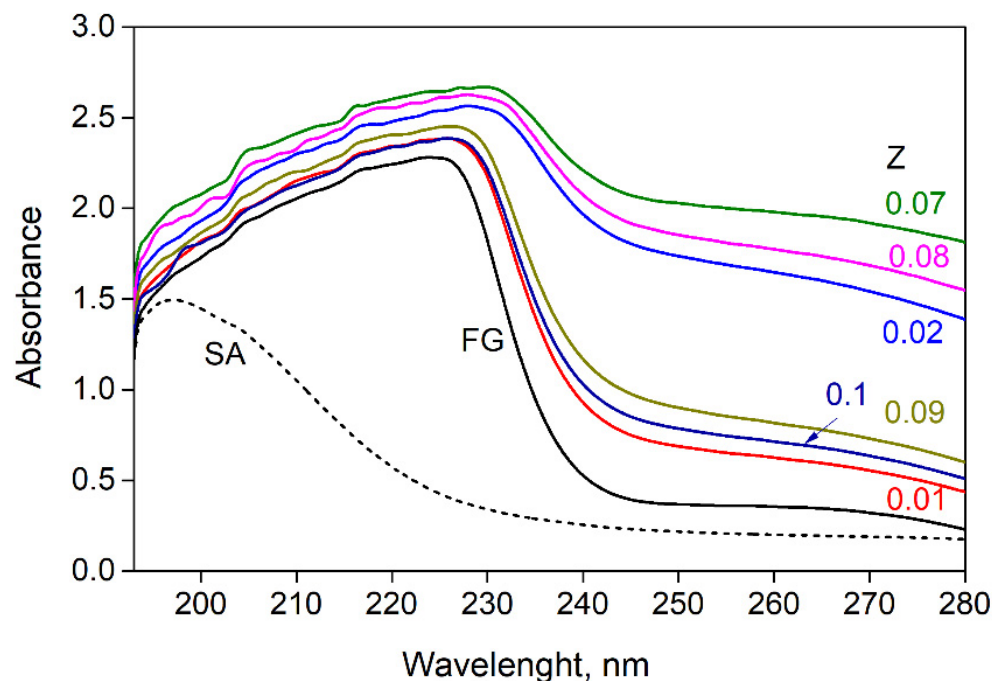


Figure 2. UV absorption spectra for sodium alginate ($C_{SA} = 0.2$ wt%), gelatin ($C_{FG} = 0.2$ wt%), and SA-FG aqueous mixtures with varying mass ratios Z .

The dependence of absorbance on the mass ratio of sodium alginate and fish gelatin was obtained (Figure 3). An increase in absorbance up to $Z \leq 0.07$ is associated with an increase in the content of stoichiometric insoluble SA-FG complexes. During the formation of stoichiometric complexes, negatively charged sodium alginate molecules are completely masked by positively charged gelatin. These complexes exist in the system together with unbound macromolecules of gelatin. The observed maximum value at $Z = 0.07$ on the curve corresponds to the formation of the maximum observed number of stoichiometric complexes as a result of the mutual neutralization of charges and the most effective formation of ionic pairs. A further increase in Z led to a decrease in the optical density of mixtures due to the formation of soluble, nonstoichiometric sodium alginate–gelatin complexes of variable composition. With an increase in the content of sodium alginate, its negative charge becomes uncompensated, which leads to an increase in complex dissolution and a decrease in absorbance.

The zeta potential of SA-FG complexes was measured to better understand the effects of the SA-FG mass ratio on the electrostatic interactions between FG and SA. The zeta potential of the mixtures was between 9.06 and -4.47 mV in the range of SA-FG mass ratio values from 0.01 to 0.10 (Figure 4a). A decrease in the zeta potential, whose value was generally between the values of pure FG (9.24 mV) and SA (-14.66 mV), with an increase in Z indicates the charge compensation between FG and AL molecules. However, the value of the zeta potential did not approach zero at $Z = 0.07$; therefore, complete neutralization of charges at this value is not observed. This may indicate that the maximum absorbance observed in Figure 3 is associated with an increase in the electrostatic interaction between SA and FG, which led to the formation of larger light-scattering aggregates. Indeed, as can be seen from Figure 4b, the maximum value of the average hydrodynamic radius (379 nm) is observed at $Z = 0.07$.

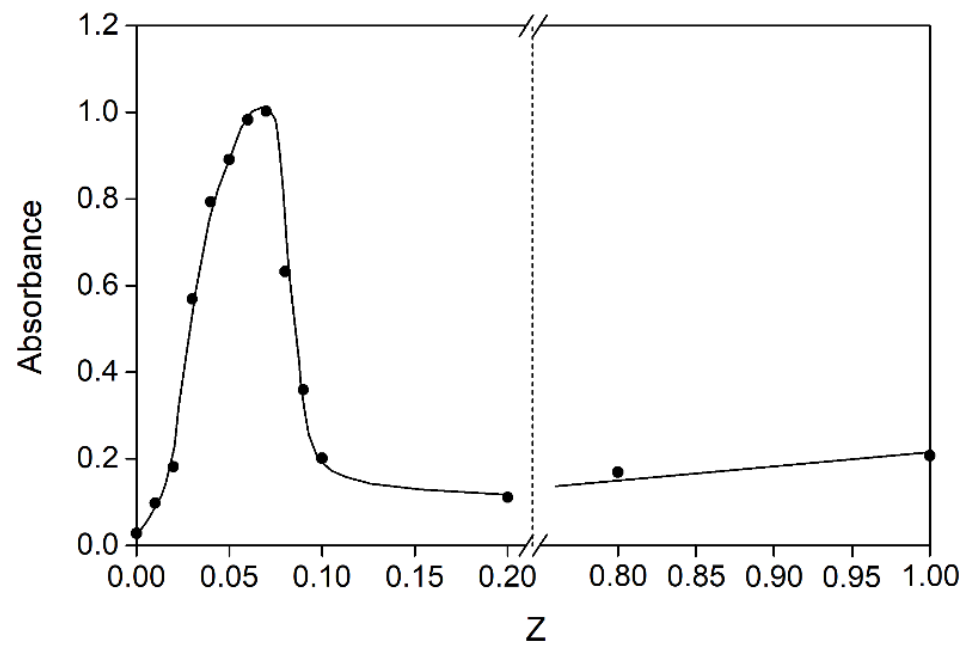


Figure 3. Absorbance as a function of SA-FG mass ratio in the titration of fish gelatin sol ($C_{FG} = 0.2\%$) with SA sol ($C_{SA} = 0.2\%$); $\lambda = 400$ nm, $l = 1$ cm, 25 °C.

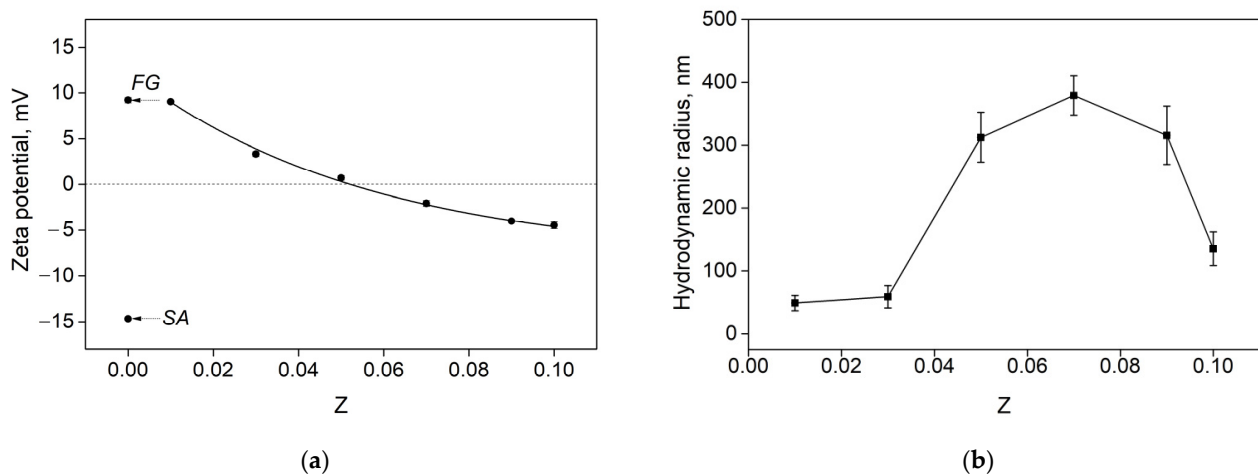


Figure 4. Changes in (a) zeta potential and (b) average hydrodynamic radius of particles for aqueous SA-FG mixtures prepared at different SA-FG values at 25 °C. pH ~ 6 .

3.2. Influence of pH

The phase behavior of SA-FG aqueous mixtures depends largely on the pH of the medium, the value of which affects, in turn, the degree of ionization of the biopolymers [17,22,23]. Figure 5a shows the UV spectra obtained for SA-FG aqueous mixtures at different pH values and $Z = 0.07$, at which the maximum value of optical density was observed. It can be seen that there is practically no shift in the absorption maximum in the pH range of 6 to 7. In this pH range, gelatin is predominantly negatively charged, although it carries a positive charge, and aqueous mixtures of SA-FG are transparent single-phase systems that contain individual molecules of biopolymers and their soluble complexes, which are formed due to the weak electrostatic interaction between the positive charge areas of the gelatin molecule and the negatively charged groups of sodium alginate molecules. However, the electrostatic repulsion between the molecular chains is greater than the electrostatic interaction. When the pH is decreased from 5 to 2, there is a significant shift in the absorption maximum from 212 to 237 nm (Figure 5b). At these pH values, gelatin is predominantly positively charged;

hence, there is stronger electrostatic interaction between gelatin and sodium alginate. As a result, insoluble complexes are formed, which separate into distinct phases, and complex coacervation is thus observed.

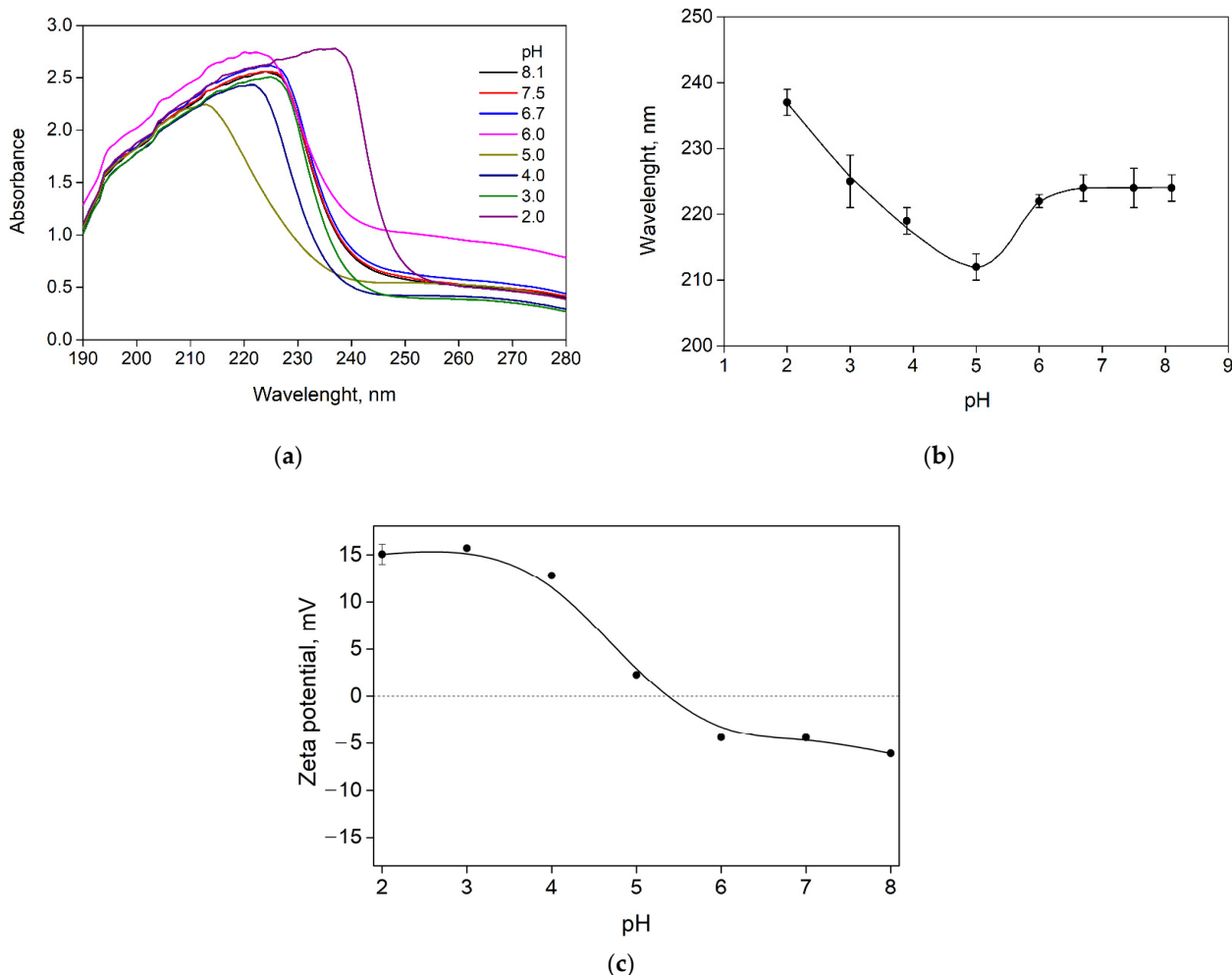


Figure 5. (a) UV absorption spectra for aqueous SA-FG mixtures prepared at different pH values and $Z = 0.07$; changes in (b) maximum absorbance and (c) zeta potential during acid titration of the SA-FG mixture prepared at $Z = 0.07$. $T = 25\text{ }^{\circ}\text{C}$.

The zeta potential of the SA-FG aqueous mixtures increased with decreasing pH from 8 to 2 due to the charge compensation between SA and FG molecules (Figure 5c). The SA-FG complexes are recharged in the pH range of 6 to 5, as evidenced by the change in the zeta potential from -4.39 to 2.30 mV, respectively. Consequently, in this pH range, there is almost complete neutralization of charges and the formation of insoluble complexes.

Figure 6 shows the dependence of the optical density of aqueous mixtures of gelatin and sodium alginate on pH obtained during acid titration. It can be seen that with an increasing mass ratio, Z , i.e., an increase in the content of sodium alginate in the system, the maximal optical density shifts to the acidic region of pH, and the system turbidity also increases. The increase in absorbance is connected with the formation of insoluble SA-FG complexes. At a pH corresponding to the curve maxima, the highest number of insoluble sodium alginate–gelatin complexes form as a result of strong electrostatic interactions between the positively charged amino groups of gelatin and the negatively charged carboxyl groups of sodium alginate. As the pH further decreases, a drop in the absorbance values is observed. This is due to the fact that the pH decrease causes protonation of carboxyl groups present in the sodium alginate molecule, which leads to a

decrease in the total charge in the sodium alginate molecule, which leads to the fewer and weaker interactions between biopolymers [18,30].

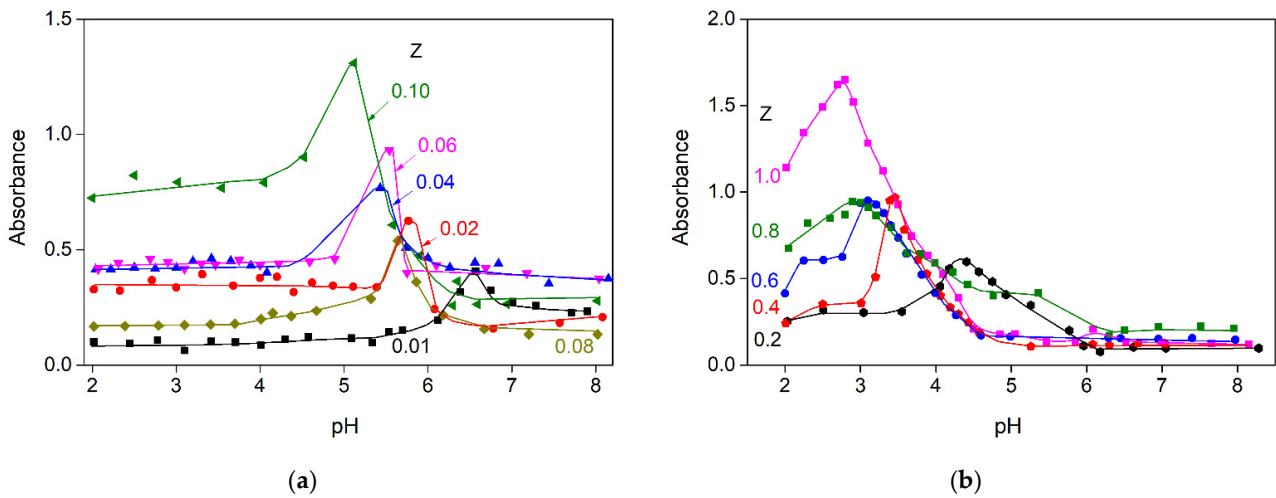


Figure 6. Changes in absorbance during the acid titration of aqueous SA-FG mixtures prepared at different Z values: (a) 0.01–0.10; (b) 0.1–1.0. $\lambda = 400$, $T = 25$ °C.

Four types of critical values of pH (pH_c , pH_{φ_1} , pH_{opt} , pH_{φ_2}) can be graphically defined regarding the dependence of optical density on the pH. The dependence of critical pH values on Z for systems containing fish gelatin and sodium alginate is shown in Figure 7.

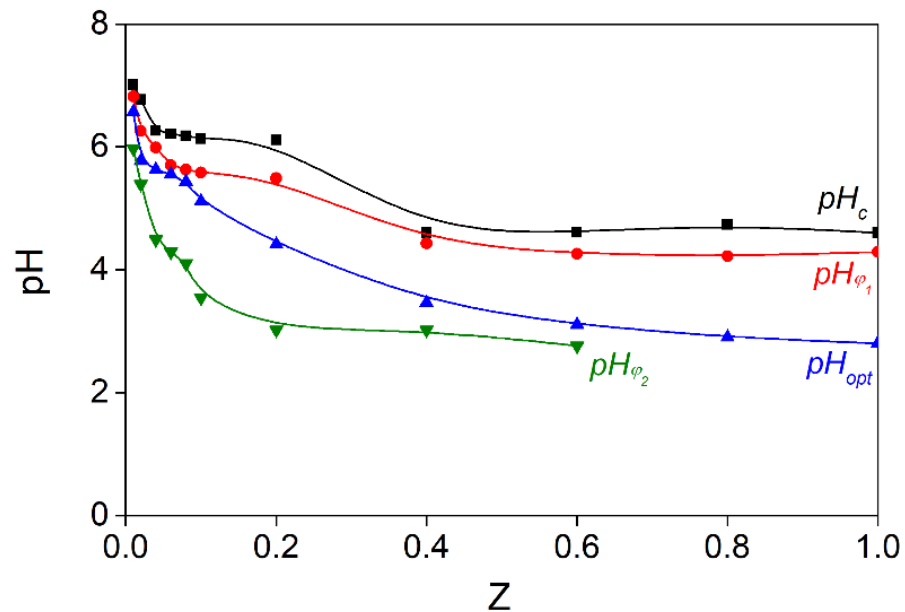


Figure 7. Changes in critical pH values during acid titration of aqueous SA-FG mixtures prepared at different Z values and $T = 25$ °C.

As can be seen in Figure 7, the values of pH_c , pH_{φ_1} , pH_{opt} , and pH_{φ_2} depend on the mass ratio of the components in the system. As Z increases from 0.08 to 1, a drop in the critical pH values is observed. Thus, as Z increases in the SA-FG mass ratio range from 0.01 to 1.00, the pH_c , pH_{φ_1} , pH_{opt} , and pH_{φ_2} values shift to a more acidic region: from 7.0 to 4.6, from 6.8 to 4.3, from 6.6 to 2.8, and from 6.0 to 2.7, respectively.

In the pH range from 8.0 to pH_{φ_1} , SA and FG co-dissolve. As the pH decreases from pH_c to pH_{φ_1} , soluble complexes are formed in SA-FG aqueous mixtures due to the weak electrostatic interactions of FG with SA. Thus, the system is a single-phase system in which

individual negatively charged sodium alginate molecules and soluble SA-FG complexes are present. In the range of $\text{pH}_{\varphi 1}$ and $\text{pH}_{\varphi 2}$, the phenomenon of complex coacervation is observed. As a result of the strong electrostatic interaction of biopolymers—wherein the conditions are optimal for biopolymer interactions with neutralized charges—insoluble complexes are formed. In this case, mixtures of sodium alginate with gelatin represent a two-phase system in which one phase is represented by molecules of the dissolving agent, and the other phase is enriched by SA-FG complexes. In the range from $\text{pH}_{\varphi 1}$ to $\text{pH}_{\varphi 2}$, the SA-FG complexes visibly aggregate. Below $\text{pH}_{\varphi 2}$, dissociation of the alginate–sodium gelatin complexes are observed as the sodium alginate chains become increasingly protonated.

Thus, a gradual decrease in pH allows gelatin to neutralize the charge of sodium alginate because an increase in the charge of gelatin increases its binding to the polyelectrolyte. Thus, the complex charge approaches a neutral value. This contributes to increased associations and, eventually, to phase separation.

TEM and SEM images were also captured to study the effect of pH on the structure of SA-FG complexes at $Z = 0.07$ with a total FG concentration of 0.1% (Figure 8). TEM images revealed that the maximum number of complex particles was observed at $\text{pH} = 5.5$ with a minimum particle size (Figure 8a). At $\text{pH} 4.5$, the number of particles decreased significantly due to the dissociation of the complexes (Figure 8b).

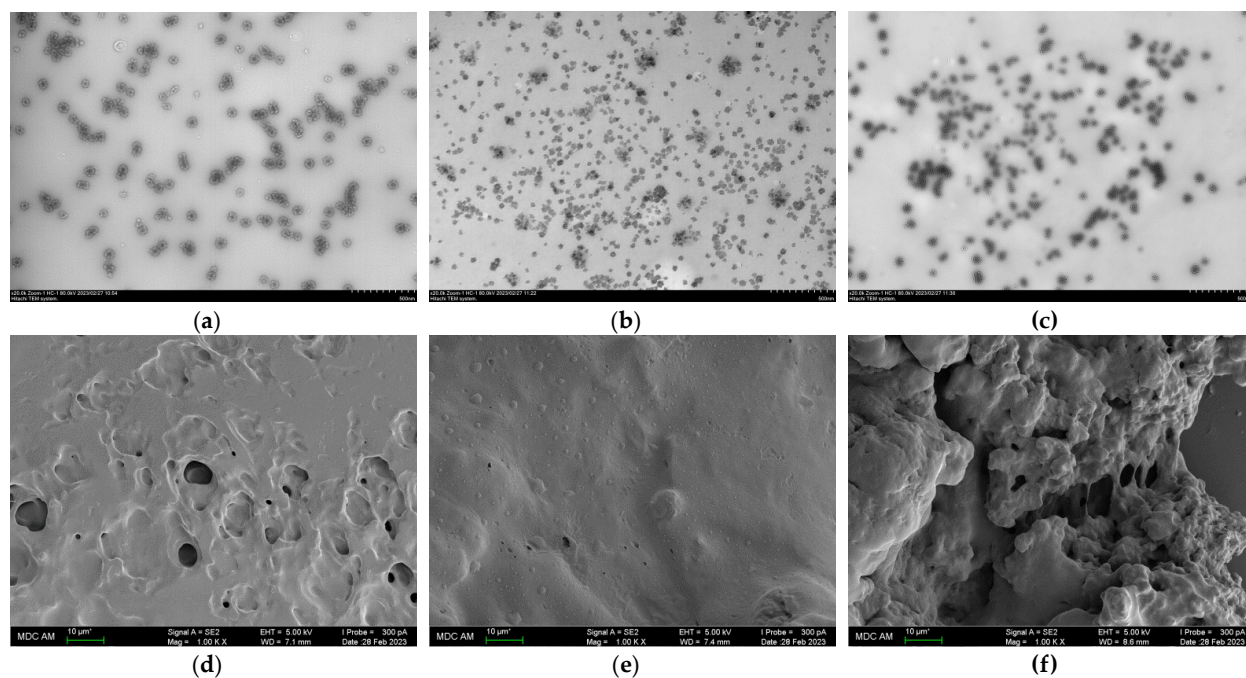


Figure 8. (a–c) TEM images of polymer-pure phase and (d–f) SEM images of SA-FG coacervates prepared at $Z = 0.07$ at different pH: (a,d) $\text{pH} = 4.5$; (b,e) $\text{pH} = 5.5$; (c,f) $\text{pH} = 6.0$. $Z = 0.07$.

The analysis of SEM images allows us to conclude that complex coacervates have different structures. The most homogeneous surface, characterized by the inclusion of small spherical particles (0.1–4 μm), is observed at $\text{pH} = 5.5$ (Figure 8e). At $\text{pH} = 4.5$, oval cavities ranging in size from 1 to 8 μm are observed on the surface of the coacervate phase (Figure 8d). The least homogeneous, friable structure is characteristic of the system obtained at $\text{pH} = 6.0$ (Figure 8f).

3.3. Influence of Ionic Strength and Cation Type

The presence of salts in the protein–polysaccharide system can result in decreased electrostatic interaction between protein and polysaccharide due to masking of the total charge carried by macromolecules, which leads to a decrease in the degree of complexation [48,49]. The effect of ionic strength on the interaction of gelatin and sodium alginate

during acid titration was studied in aqueous solutions of sodium and calcium chlorides. The NaCl and CaCl₂ concentration was varied from 1 to 200 mM at a mass ratio of $Z = 0.07$ and a gelatin concentration of 0.1% wt.

We found that the presence of electrolytes has a strong influence on the phase behavior of aqueous mixtures of sodium alginate with fish gelatin (Figure 9). As the concentration of the electrolyte increases, the absorbance decreases, and the peak position shifts to more acidic pH values. At NaCl concentrations from 1 to 10 mM, formation of the coacervate phase was observed, although the release of insoluble sodium alginate coacervates with gelatin occurred at lower pH values compared with the system containing no electrolyte ($C(\text{NaCl}) = 0$). At sodium chloride concentrations from 50 to 200 mM, no phase coacervation was observed, and the system is a transparent single-phase, which is indicative of almost complete suppression of the electrostatic interaction between gelatin and sodium alginate molecules because the increase in ionic strength led to an accompanying increase in the condensation of low-molecular counterions on the biopolymer surface. When NaCl was added to the SA-FG aqueous mixtures, the critical pH values (pH_c , $\text{pH}_{\varphi 1}$, pH_{opt} , $\text{pH}_{\varphi 2}$) shifted toward lower values (Figure 9a). This shift in the critical pH values is explained by the shielding effect of NaCl on sodium alginate and gelatin. CaCl₂ caused even greater suppression of the interaction between SA and FG due to the larger cation radius (Figure 9b).

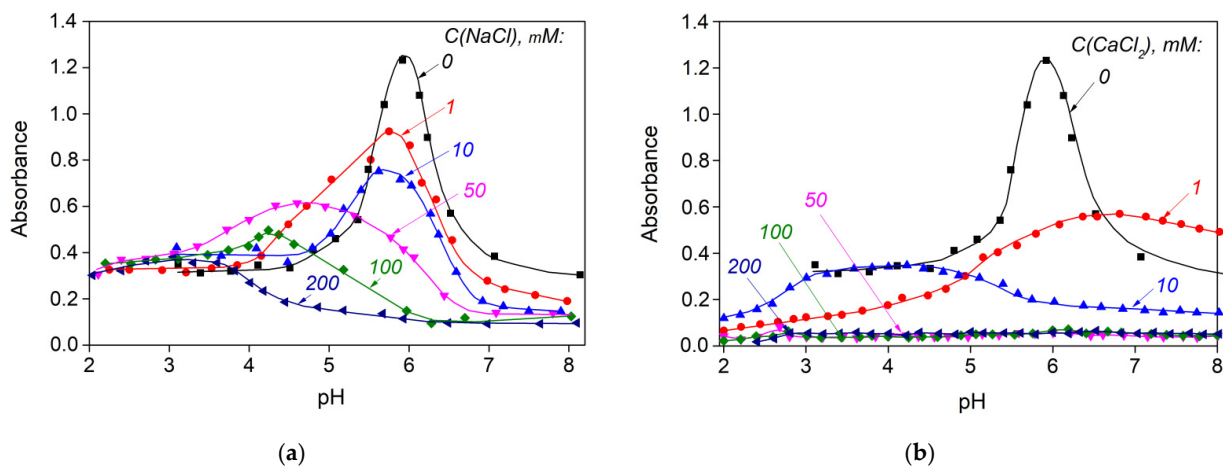


Figure 9. Changes in absorbance during the acid titration of aqueous SA-FG mixtures prepared at different concentrations of (a) NaCl and (b) CaCl₂, where $Z = 0.07$, $\lambda = 400$, and $T = 25\text{ }^{\circ}\text{C}$.

Complexation occurs only when gelatin is sufficiently protonated at lower pH values. It should be noted that the absorption maximum also decreases as the electrolyte concentration increases. Similar effects were observed for systems containing fish gelatin and sodium alginate [17], whey protein and carrageenan [50], bovine whey albumin and pectin [51], and pea protein isolate and hummarabic [52].

4. Conclusions

The results of this study indicate that SA-FG aqueous mixtures exhibit different phase behaviors depending on the pH and ionic strength. During acid titration, it was shown that, as the mass ratio of the components (Z) was increased from 0.01 to 1.00, the turbidity of the system increased, and the optical density maximum shifted to the acidic region from pH 6.6 to 2.8. A decrease in pH induces complex coacervation in SA-FG aqueous mixtures. In the pH range from 8.0 to $\text{pH}_{\varphi 1}$, aqueous SA-FG mixtures represent a single-phase system containing single negatively charged SA molecules and soluble SA-FG complexes that form due to weak electrostatic interactions. In the $\text{pH}_{\varphi 1}$ to $\text{pH}_{\varphi 2}$ range, a biphasic system is formed in which one of the phases consists of insoluble SA-FG complexes. The maximum observed interaction between SA and FG occurs at pH_{opt} , and a further decrease in pH to

$\text{pH}_{\varphi 2}$ causes visible aggregation of SA-FG complexes. Below $\text{pH}_{\varphi 2}$, complex disassociation occurs as the SA chains become increasingly protonated.

With an increase in SA-FG mass ratios from 0.01 to 1.00, the boundary values of pH_c , $\text{pH}_{\varphi 1}$, pH_{opt} , and $\text{pH}_{\varphi 2}$ become more acidic: shifting from 7.0 to 4.6, from 6.8 to 4.3, from 6.6 to 2.8, and from 6.0 to 2.7, respectively.

The addition of NaCl or CaCl_2 leads to suppression of the electrostatic -interaction between gelatin and sodium alginate molecules, whereas interaction is suppressed almost completely at high concentrations of NaCl or CaCl_2 (100 and 200 mM), and no coacervation occurs in the SA-FG system.

Understanding the phase behavior and patterns of complex formation in aqueous mixtures of SA-FG will allow the physical and chemical properties of polyelectrolyte complexes of SA-FG to be regulated in order to obtain compositions for developing new functional materials for different applications, such as encapsulation, textural modification, and stabilization in food systems.

Author Contributions: Conceptualization, D.S.K. and S.R.D.; methodology, D.S.K.; validation, D.S.K. and S.R.D.; formal analysis, D.S.K.; investigation, D.S.K., E.V.B., V.V.B., V.V.S., Y.F.Z. and O.S.Z.; writing—original draft preparation, D.S.K.; writing—review and editing, D.S.K. and S.R.D.; visualization, D.S.K.; supervision, D.S.K.; project administration, D.S.K. and S.R.D. All authors have read and agreed to the published version of the manuscript.

Funding: This research was funded by the Russian Science Foundation, project no. 21-73-00191.

Institutional Review Board Statement: Not applicable.

Informed Consent Statement: Not applicable.

Data Availability Statement: Not applicable.

Acknowledgments: D.S.K. is grateful to the Russian Ministry of Science and Higher Education for the support of the Laboratory of Chemistry and Technology of Marine Bioresources founded as part of the national project “Science and Universities” (Agreement № 075-03-2021-088/4). S.R.D. thanks for the support of the Russian Science Foundation (project no. 22-16-20046). V.V.S. and Y.F.Z. give thanks for financial support from the government assignment for the FRC Kazan Scientific Center of RAS. The contribution of Y.F.Z. was partly supported by the Kazan Federal University Strategic Academic Leadership Program (“PRIORITY-2030”). O.S.Z. gives thanks for the support of the Kazan State Power Engineering University Strategic Academic Leadership Program (“PRIORITY-2030”). Scanning electron microscopy investigation was performed using the equipment of the Interdisciplinary Center “Analytical Microscopy” (Kazan Federal University, Kazan, Russia). Transmission electron microscopy study has been carried out using the equipment of Distributed Spectral-Analytical Center of Shared Facilities for Study of Structure, Composition and Properties of Substances and Materials of FRC Kazan Scientific Center of RAS. Experimental research on turbidimetric and UV absorption spectrum measurements, turbidimetric acid titration, particle size, and zeta potential measurements was carried out with the support of the Russian Science Foundation, project no. 21-73-00191.

Conflicts of Interest: The authors declare no conflict of interest. The funders had no role in the design of the study; in the collection, analyses, or interpretation of data; in the writing of the manuscript; or in the decision to publish the results.

References

1. Li, H.; Wang, T.; Hu, Y.; Wu, J.; van der Meeren, P. Designing Delivery Systems for Functional Ingredients by Protein/Polysaccharide Interactions. *Trends Food Sci. Technol.* **2022**, *119*, 272–287. [[CrossRef](#)]
2. Fan, Z.; Cheng, P.; Zhang, P.; Zhang, G.; Han, J. Rheological Insight of Polysaccharide/Protein Based Hydrogels in Recent Food and Biomedical Fields: A Review. *Int. J. Biol. Macromol.* **2022**, *222*, 1642–1664. [[CrossRef](#)] [[PubMed](#)]
3. Devi, N.; Sarmah, M.; Khatun, B.; Maji, T.K. Encapsulation of Active Ingredients in Polysaccharide–Protein Complex Coacervates. *Adv. Colloid Interface Sci.* **2017**, *239*, 136–145. [[CrossRef](#)]
4. Cai, Z.; Wei, Y.; Shi, A.; Zhong, J.; Rao, P.; Wang, Q.; Zhang, H. Correlation between Interfacial Layer Properties and Physical Stability of Food Emulsions: Current Trends, Challenges, Strategies, and Further Perspectives. *Adv. Colloid Interface Sci.* **2023**, *313*, 102863. [[CrossRef](#)]

5. Falsafi, S.R.; Rostamabadi, H.; Samborska, K.; Mirarab, S.; Rashidinejad, A.; Jafari, S.M. Protein-Polysaccharide Interactions for the Fabrication of Bioactive-Loaded Nanocarriers: Chemical Conjugates and Physical Complexes. *Pharmacol. Res.* **2022**, *178*, 106164. [[CrossRef](#)] [[PubMed](#)]
6. Pascuta, M.S.; Varvara, R.-A.; Teleky, B.-E.; Szabo, K.; Plamada, D.; Nemeş, S.-A.; Mitrea, L.; Martău, G.A.; Ciont, C.; Călinoiu, L.F.; et al. Polysaccharide-Based Edible Gels as Functional Ingredients: Characterization, Applicability, and Human Health Benefits. *Gels* **2022**, *8*, 524. [[CrossRef](#)]
7. Rosellini, E.; Zhang, Y.S.; Migliori, B.; Barbani, N.; Lazzeri, L.; Shin, S.R.; Dokmeci, M.R.; Cascone, M.G. Protein/Polysaccharide-Based Scaffolds Mimicking Native Extracellular Matrix for Cardiac Tissue Engineering Applications. *J. Biomed. Mater. Res. Part A* **2018**, *106*, 769–781. [[CrossRef](#)]
8. Lafarga, T.; Acien-Fernández, F.G.; Garcia-Vaquero, M. Bioactive Peptides and Carbohydrates from Seaweed for Food Applications: Natural Occurrence, Isolation, Purification, and Identification. *Algal Res.* **2020**, *48*, 101909. [[CrossRef](#)]
9. Yada, R.Y. *Proteins in Food Processing*; Woodhead Publishing: Sawston, UK, 2017; ISBN 978-0-08-100729-7.
10. Hong, S.; Choi, D.W.; Kim, H.N.; Park, C.G.; Lee, W.; Park, H.H. Protein-Based Nanoparticles as Drug Delivery Systems. *Pharmaceutics* **2020**, *12*, 604. [[CrossRef](#)]
11. Chen, H.; Wang, J.; Cheng, Y.; Wang, C.; Liu, H.; Bian, H.; Pan, Y.; Sun, J.; Han, W. Application of Protein-Based Films and Coatings for Food Packaging: A Review. *Polymers* **2019**, *11*, 2039. [[CrossRef](#)]
12. Wang, L.-S.; Gopalakrishnan, S.; Luther, D.C.; Rotello, V.M. Protein-Based Films as Antifouling and Drug-Eluting Antimicrobial Coatings for Medical Implants. *ACS Appl. Mater. Interfaces* **2021**, *13*, 48301–48307. [[CrossRef](#)] [[PubMed](#)]
13. Sionkowska, A.; Adamiak, K.; Musiał, K.; Gadomska, M. Collagen Based Materials in Cosmetic Applications: A Review. *Materials* **2020**, *13*, 4217. [[CrossRef](#)] [[PubMed](#)]
14. Shao, P.; Feng, J.; Sun, P.; Xiang, N.; Lu, B.; Qiu, D. Recent Advances in Improving Stability of Food Emulsion by Plant Polysaccharides. *Food Res. Int.* **2020**, *137*, 109376. [[CrossRef](#)] [[PubMed](#)]
15. Muthukumar, J.; Chidambaram, R.; Sukumaran, S. Sulfated Polysaccharides and Its Commercial Applications in Food Industries—A Review. *J. Food Sci. Technol.* **2021**, *58*, 2453–2466. [[CrossRef](#)]
16. Mohammed, A.S.A.; Naveed, M.; Jost, N. Polysaccharides; Classification, Chemical Properties, and Future Perspective Applications in Fields of Pharmacology and Biological Medicine (A Review of Current Applications and Upcoming Potentialities). *J. Polym. Environ.* **2021**, *29*, 2359–2371. [[CrossRef](#)]
17. Razzak, M.A.; Kim, M.; Chung, D. Elucidation of Aqueous Interactions between Fish Gelatin and Sodium Alginate. *Carbohydr. Polym.* **2016**, *148*, 181–188. [[CrossRef](#)]
18. Chung, D. Chapter 3—Fish Gelatin: Molecular Interactions and Applications. In *Biopolymer-Based Formulations*; Pal, K., Banerjee, I., Sarkar, P., Kim, D., Deng, W.-P., Dubey, N.K., Majumder, K., Eds.; Elsevier: Amsterdam, The Netherlands, 2020; pp. 67–85. ISBN 978-0-12-816897-4.
19. McClements, D.J. Non-Covalent Interactions between Proteins and Polysaccharides. *Biotechnol. Adv.* **2006**, *24*, 621–625. [[CrossRef](#)]
20. Schmitt, C.; Aberkane, L.; Sanchez, C. 16—Protein–Polysaccharide Complexes and Coacervates. In *Handbook of Hydrocolloids*, 2nd ed.; Phillips, G.O., Williams, P.A., Eds.; Woodhead Publishing Series in Food Science, Technology and Nutrition; Woodhead Publishing: Sawston, UK, 2009; pp. 420–476. ISBN 978-1-84569-414-2.
21. Turgeon, S.L.; Laneville, S.I. Chapter 11—Protein + Polysaccharide Coacervates and Complexes: From Scientific Background to Their Application as Functional Ingredients in Food Products. In *Modern Biopolymer Science*; Kasapis, S., Norton, I.T., Ubbink, J.B., Eds.; Academic Press: San Diego, CA, USA, 2009; pp. 327–363. ISBN 978-0-12-374195-0.
22. Shi, X.-D.; Huang, J.-J.; Wu, J.-L.; Cai, X.-X.; Tian, Y.-Q.; Rao, P.-F.; Huang, J.-L.; Wang, S.-Y. Fabrication, Interaction Mechanism, Functional Properties, and Applications of Fish Gelatin-Polysaccharide Composites: A Review. *Food Hydrocoll.* **2022**, *122*, 107106. [[CrossRef](#)]
23. Razzak, M.A.; Kim, M.; Kim, H.-J.; Park, Y.-C.; Chung, D. Deciphering the Interactions of Fish Gelatine and Hyaluronic Acid in Aqueous Solutions. *Int. J. Biol. Macromol.* **2017**, *102*, 885–892. [[CrossRef](#)]
24. Harnsilawat, T.; Pongsawatmanit, R.; McClements, D.J. Characterization of β -Lactoglobulin–Sodium Alginate Interactions in Aqueous Solutions: A Calorimetry, Light Scattering, Electrophoretic Mobility and Solubility Study. *Food Hydrocoll.* **2006**, *20*, 577–585. [[CrossRef](#)]
25. Phawaphuthanon, N.; Yu, D.; Ngamnikom, P.; Shin, I.-S.; Chung, D. Effect of Fish Gelatine-Sodium Alginate Interactions on Foam Formation and Stability. *Food Hydrocoll.* **2019**, *88*, 119–126. [[CrossRef](#)]
26. Xue, J.; Luo, Y. Protein-Polysaccharide Nanocomplexes as Nanocarriers for Delivery of Curcumin: A Comprehensive Review on Preparation Methods and Encapsulation Mechanisms. *J. Future Foods* **2023**, *3*, 99–114. [[CrossRef](#)]
27. Zhang, Q.; Zhou, Y.; Yue, W.; Qin, W.; Dong, H.; Vasanthan, T. Nanostructures of Protein-Polysaccharide Complexes or Conjugates for Encapsulation of Bioactive Compounds. *Trends Food Sci. Technol.* **2021**, *109*, 169–196. [[CrossRef](#)]
28. Zheng, T. Improving Absorption and Bioactivities of Phytochemicals Using Protein/Polysaccharide Nanoparticle Delivery Systems. Ph.D. Thesis, Rutgers University—School of Graduate Studies, New Brunswick, NJ, USA, 2022. [[CrossRef](#)]
29. Lankalapalli, S.; Kolapalli, V.R. Polyelectrolyte Complexes: A Review of Their Applicability in Drug Delivery Technology. *Indian J. Pharm. Sci.* **2009**, *71*, 481. [[CrossRef](#)] [[PubMed](#)]
30. Sarika, P.R.; Pavithran, A.; James, N.R. Cationized Gelatin/Gum Arabic Polyelectrolyte Complex: Study of Electrostatic Interactions. *Food Hydrocoll.* **2015**, *49*, 176–182. [[CrossRef](#)]

31. Wagoner, T.B.; Foegeding, E.A. Whey Protein–Pectin Soluble Complexes for Beverage Applications. *Food Hydrocoll.* **2017**, *63*, 130–138. [[CrossRef](#)]
32. Setiowati, A.D.; Saeedi, S.; Wijaya, W.; van der Meeren, P. Improved Heat Stability of Whey Protein Isolate Stabilized Emulsions via Dry Heat Treatment of WPI and Low Methoxyl Pectin: Effect of Pectin Concentration, PH, and Ionic Strength. *Food Hydrocoll.* **2017**, *63*, 716–726. [[CrossRef](#)]
33. Stone, A.K.; Cheung, L.; Chang, C.; Nickerson, M.T. Formation and Functionality of Soluble and Insoluble Electrostatic Complexes within Mixtures of Canola Protein Isolate and (κ -, ι - and λ -Type) Carrageenan. *Food Res. Int.* **2013**, *54*, 195–202. [[CrossRef](#)]
34. Schmitt, C.; Turgeon, S.L. Protein/Polysaccharide Complexes and Coacervates in Food Systems. *Adv. Colloid Interface Sci.* **2011**, *167*, 63–70. [[CrossRef](#)]
35. Scholten, E.; Moschakis, T.; Biliaderis, C.G. Biopolymer Composites for Engineering Food Structures to Control Product Functionality. *Food Struct.* **2014**, *1*, 39–54. [[CrossRef](#)]
36. Liu, S.; Elmer, C.; Low, N.H.; Nickerson, M.T. Effect of PH on the Functional Behaviour of Pea Protein Isolate–Gum Arabic Complexes. *Food Res. Int.* **2010**, *43*, 489–495. [[CrossRef](#)]
37. Rather, J.A.; Akhter, N.; Ashraf, Q.S.; Mir, S.A.; Makroo, H.A.; Majid, D.; Barba, F.J.; Khaneghah, A.M.; Dar, B.N. A Comprehensive Review on Gelatin: Understanding Impact of the Sources, Extraction Methods, and Modifications on Potential Packaging Applications. *Food Packag. Shelf Life* **2022**, *34*, 100945. [[CrossRef](#)]
38. Siburian, W.Z.; Rochima, E.; Andriani, Y.; Praseptiangga, D. Fish Gelatin (Definition, Manufacture, Analysis of Quality Characteristics, and Application): A Review. *Int. J. Fish. Aquat. Stud.* **2020**, *8*, 90–95.
39. Szekalska, M.; Puciłowska, A.; Szymańska, E.; Ciosek, P.; Winnicka, K. Alginate: Current Use and Future Perspectives in Pharmaceutical and Biomedical Applications. *Int. J. Polym. Sci.* **2016**, *2016*, e7697031. [[CrossRef](#)]
40. Li, Y.; Jia, H.; Cheng, Q.; Pan, F.; Jiang, Z. Sodium Alginate–Gelatin Polyelectrolyte Complex Membranes with Both High Water Vapor Permeance and High Permselectivity. *J. Membr. Sci.* **2011**, *375*, 304–312. [[CrossRef](#)]
41. Tong, L.; Kang, X.; Fang, Q.; Yang, W.; Cen, S.; Lou, Q.; Huang, T. Rheological Properties and Interactions of Fish Gelatin–K-carrageenan Polyelectrolyte Hydrogels: The Effects of Salt. *J. Texture Stud.* **2022**, *53*, 122–132. [[CrossRef](#)] [[PubMed](#)]
42. Zorzi, G.K.; Párraga, J.E.; Seijo, B.; Sánchez, A. Hybrid Nanoparticle Design Based on Cationized Gelatin and the Polyanions Dextran Sulfate and Chondroitin Sulfate for Ocular Gene Therapy. *Macromol. Biosci.* **2011**, *11*, 905–913. [[CrossRef](#)]
43. Golovchenko, V.V.; Bushneva, O.A.; Ovodova, R.G.; Shashkov, A.S.; Chizhov, A.O.; Ovodov, Y.S. Structural Study of Bergenin, a Pectin from *Bergenina Crassifolia*. *Russ. J. Bioorg. Chem.* **2007**, *33*, 47–56. [[CrossRef](#)]
44. Usov, A.I.; Bilan, M.I.; Klochkova, N.G. Polysaccharides of Algae. 48. Polysaccharide Composition of Several Calcareous Red Algae: Isolation of Alginate from *Corallina pilulifera* P. et R. (Rhodophyta, Corallinaceae). *Bot. Mar.* **1995**, *38*, 43–52. [[CrossRef](#)]
45. Derkach, S.R.; Kuchina, Y.A.; Baryshnikov, A.V.; Kolotova, D.S.; Voron'ko, N.G. Tailoring Cod Gelatin Structure and Physical Properties with Acid and Alkaline Extraction. *Polymers* **2019**, *11*, 1724. [[CrossRef](#)]
46. Rabek, J.F. *Experimental Methods in Polymer Chemistry: Physical Principles and Applications*; John Wiley & Sons, Inc.: New York, NY, USA, 1980.
47. Lundblad, R.L.; Macdonald, F.M. *Handbook of Biochemistry and Molecular Biology*; CRC Press: Boca Raton, FL, USA, 2010.
48. Zhang, J.; Du, H.; Ma, N.; Zhong, L.; Ma, G.; Pei, F.; Chen, H.; Hu, Q. Effect of Ionic Strength and Mixing Ratio on Complex Coacervation of Soy Protein Isolate/Flammulina Velutipes Polysaccharide. *Food Sci. Hum. Wellness* **2023**, *12*, 183–191. [[CrossRef](#)]
49. Han, J.; Yan, J.; Du, Y.; Wu, H.; Zhu, B. Formation and Stability of Electrostatic Complexes Formed between Scallop Female Gonad Protein Isolates and Sodium Alginate: Influence of PH, Total Concentration, Blend Ratio, and Ionic Strength. *J. Food Sci.* **2022**, *87*, 2504–2514. [[CrossRef](#)]
50. Weinbreck, F.; Nieuwenhuijse, H.; Robijn, G.W.; de Kruif, C.G. Complexation of Whey Proteins with Carrageenan. *J. Agric. Food Chem.* **2004**, *52*, 3550–3555. [[CrossRef](#)] [[PubMed](#)]
51. Li, X.; Fang, Y.; Al-Assaf, S.; Phillips, G.O.; Yao, X.; Zhang, Y.; Zhao, M.; Zhang, K.; Jiang, F. Complexation of Bovine Serum Albumin and Sugar Beet Pectin: Structural Transitions and Phase Diagram. *Langmuir* **2012**, *28*, 10164–10176. [[CrossRef](#)]
52. Liu, S.; Low, N.H.; Nickerson, M.T. Effect of pH, Salt, and Biopolymer Ratio on the Formation of Pea Protein Isolate–Gum Arabic Complexes. *J. Agric. Food Chem.* **2009**, *57*, 1521–1526. [[CrossRef](#)] [[PubMed](#)]

Disclaimer/Publisher's Note: The statements, opinions and data contained in all publications are solely those of the individual author(s) and contributor(s) and not of MDPI and/or the editor(s). MDPI and/or the editor(s) disclaim responsibility for any injury to people or property resulting from any ideas, methods, instructions or products referred to in the content.